JOURNAL OF CATALYSIS **121**, 318–326 (1990)

Hydrogenation and H–D Exchange of Chemisorbed Ethylene on Ni(100) under Vacuum

FRANCISCO ZAERA

Department of Chemistry, University of California, Riverside, Riverside, California 92521

Received July 6, 1989; revised September 22, 1989

Thermal desorption (TDS) and high-resolution electron energy loss (HREELS) spectroscopies have been used to study the reactivity of ethylene with coadsorbed hydrogen on Ni(100) surfaces under vacuum conditions. Hydrogen coadsorption weakens ethylene chemisorption, decreasing the activation barrier and increasing the desorption yield compared to those of the unmodified ethylene adsorption. H–D exchange in ethylene takes place to a large extent; up to 20–30% of the molecules go through at least one exchange reaction before desorbing. Ethylene hydrogenation competes with both molecular desorption and H–D exchange and is very sensitive to chemisorption geometries. The yields and energetics of all three reactions are greatly influenced by the relative coverages and the order of dosing between ethylene and hydrogen.

INTRODUCTION

A good knowledge of the reactivity of hydrocarbons on transition metal surfaces is highly desirable in designing many industrial catalytic processes. The surface chemistry of ethylene can be used as a prototype for understanding the different factors controlling the reactivity and selectivity for hydrocarbon reactions. Ethylene is an ideal choice because, despite being a simple molecule, it can undergo hydrogenation, dehydrogenation, and H–D exchange reactions. The hydrogenation of ethylene on supported catalysts has been extensively studied (*1*), and ethylene chemisorption has also been carefully characterized on several single-crystal transition metal surfaces by using a combination of modern surface-sensitive techniques (*2, 3*). On Ni(100), chemisorption takes place molecularly at liquid nitrogen temperatures, and vinyl groups form around 170 K (*4–6*). Vinyl then decomposes around 230 K to form acetylenic fragments and dehydrogenates further to CCH and surface carbon at higher temperatures (*7*).

Hydrogenation and H–D exchange reactions on single crystals have been studied to a lesser extent (*2*). It has recently been shown that the catalytic hydrogenation of ethylene under atmospheric pressures takes place in the presence of strongly adsorbed hydrocarbon fragments (ethylidyne) (*8, 9*), but the mechanism for this reaction is not fully understood (*8*). However, it is clear that the same reaction follows a different mechanism under ultrahigh vacuum (UHV) conditions (*10*). The rates for ethylene hydrogenation and self-hydrogenation have also been measured on Ni(100) and Ni(111) (*11, 12*), but little insight has been obtained regarding their mechanism. In this paper we report results on the reactivity of deuterated ethylene (C_2D_4) with hydrogen on Ni(100) under UHV. Special emphasis is given to the study of hydrogenation and H–D exchange reactions.

METHODS

The experiments were preformed in a stainless-steel ultrahigh vacuum (UHV) chamber described in detail elsewhere (*4*). Briefly, the system is equipped with a mass spectrometer for thermal desorption (TDS) experiments, a high-resolution energy loss (HREELS) spectrometer, and a hemispherical electron energy analyzer for Auger

0021-9517/90 $3.00

electron (AES) and X-ray photoelectron (XPS) spectroscopies. TDS data was acquired using a sniffer (*13*), which selectively detected desorption from the front face of the crystal. Gas exposures were done using dosers, which increased the partial pressures of the gas being dosed on the crystal face by a factor of 80 (ethylene) or 17.5 (hydrogen) with respect to the background. The mass spectrometer was computer interfaced, allowing for multiple mass detection in a single TDS experiment.

HREEL spectra were taken in a double "C" cylindrical 127° analyzer described elsewhere (*14*). An incident electron energy of 5 eV was used, with a full-width at half-maximum (FWHM) of 9 meV. Typical signals were 6–8 × 10^5 cps for the elastic peak and 1–3 × 10^2 cps for the loss features (detected in the specular direction).

The Ni single-crystal sample was oriented in the (100) plane, cut and polished using standard procedures, and mounted in a manipulator for heating and cooling and for handling inside the vacuum chamber. The crystal temperature was monitored using a chromel–alumel thermocouple spot-welded to the sample edge, and a linear temperature programmer was used in the TDS experiments in order to achieve a 10 K/s heating rate over the complete temperature range.

The deuterated ethylene was obtained from MSD isotopes (99 at.% D, isotopic purity) and was outgassed by repeated freeze–pumping cycles prior to use. The hydrogen was Matheson purity (99.9995%) and was used as supplied. The ion gauge used for pressure measurements was calibrated for differences in sensitivity for each gas (*15*); exposures reported in this work are corrected by these factors.

RESULTS

Thermal desorption spectra (TDS) for coadsorbed hydrogen and ethylene on Ni(100) are shown in Figs. 1 to 4. TDS from surfaces where either hydrogen dosing was followed by ethylene (0.85 and 10 Langmuirs, respectively, 1 Langmuir = 1 × 10^{-6} Torr · s) or ethylene dosing was followed by hydrogen (1.3 and 0.85 Langmuirs, respectively) were performed. The exposures used in these experiments were chosen in order to obtain close to half-monolayer coverages for both gases. Controlled TDS experiments were performed to determine approximate coverages. It was found that 0.85 Langmuirs of ethylene on clean Ni(100) yielded a coverage of about $\theta = 0.6$ (where $\theta = 1$ is saturation) (*4*), while for hydrogen an exposure of 0.85 Langmuirs corresponded to a coverage of about $\theta = 0.3$, (10 Langmuirs yielded saturation). However, the values given above are for cases when only one gas was adsorbed on a clean surface and could not be directly used to determine the coverages for coadsorption experiments since exposure to the second gas displaces some of the molecules adsorbed on the surface (*16*). We found, for instance, that a 1.3-Langmuirs ethylene dose followed by 10 Langmuirs of H_2 resulted in an ethylene coverage of $\theta = 0.4$, about half of the value before hydrogen exposure. We made sure that the doses chosen in our experiments guarantee appreciable coverages for both gases on the surface.

Figure 1 shows the 2(H_2)-, 3(HD)-, and 4(D_2)-amu TDS traces obtained after ethylene and hydrogen coadsorption on Ni(100). Hydrogen thermal desorption from hydrogen- and ethylene-saturated surfaces are shown on the top for reference. The hydrogen thermal desorption from adsorbed H_2 displays two peaks, one at 335 K, which populates first, and a second one at 255 K, which grows at high coverages. The TDS from ethylene also shows two peaks, one at 325 K followed by a shoulder at 400 K for high coverages (*4*). The hydrogen TDS from all coadsorption experiments look almost the same regardless of the order of adsorption. In both cases the peaks observed below 250 K are due to cracking of molecular C_2D_4 in the mass spectrometer ionizer. The 2-amu traces show two addi-

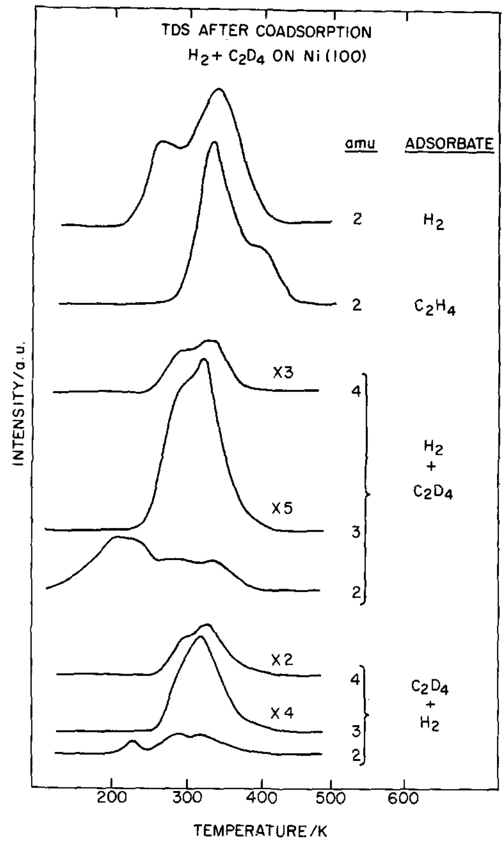

FIG. 1. Hydrogen (H_2, 2 amu; HD, 3 amu; and D_2, 4 amu) thermal desorption spectra for chemisorbed hydrogen, chemisorbed ethylene, and coadsorbed hydrogen and deuterated ethylene (H_2 followed by C_2D_4 and C_2D_4 followed by H_2) on Ni(100). T_{ads} = 90 K, heating rate = 10 K/s.

tional peaks at about 280 and 315 K, the first of which is shifted to lower temperatures for the case where H_2 is adsorbed first (270 vs 290 K). Two peaks are also seen in the 4-amu TDS, with maxima around 290 and 323 K, and are also displaced depending on the order of dosing (285 K for H_2 predosing, 292 K when starting with ethylene). The traces for HD (3 amu) have peaks at temperatures that are intermediate between those for 2 and 4 amu. The shifts in peaks between H_2, HD, and D_2 for a given system may be due to a kinetic isotope effect, but changes in the TDS spectra for the same mass between the two systems are a reflection of different surface chemistry.

TDS for 15, 16, 17, 30, 31, 32, and 34 amu obtained after hydrogen and deuterated ethylene coadsorption on Ni(100) are shown in Figs. 2 and 4. Figure 2 corresponds to the experiments where hydrogen was dosed first. The 32-amu trace, which corresponds to molecular C_2D_4, has a broad peak with maximum at 185 K and shoulders at around 220 and 260 K. The spectra for 30 and 16 amu mainly correspond to C_2D_4 also; they are similar to the one for 32 amu but scaled according to the relative intensities in the C_2D_4 cracking pattern (about 60 and 10% of the parent peak for the 30- and 16-amu signals, respectively (*17*)). Molecular desorption in this coadsorption system was similar than that for pure ethylene adsorbed on Ni(100) (*4*), but the peaks were

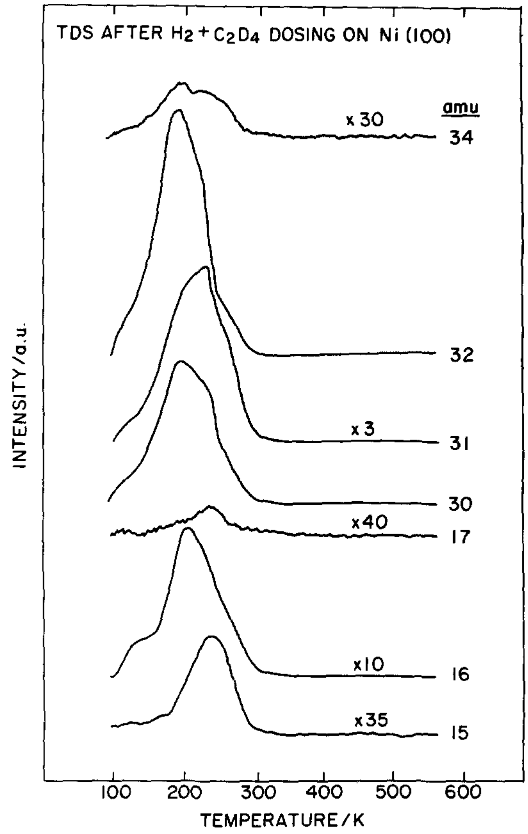

FIG. 2. TDS for 15, 16, 17, 30, 31, 32, and 34 amu after dosing sequentially a Ni(100) surface with 0.85 Langmuirs H_2 followed by 10 Langmuirs C_2D_4 at 90 K. Heating rate = 10 K/s.

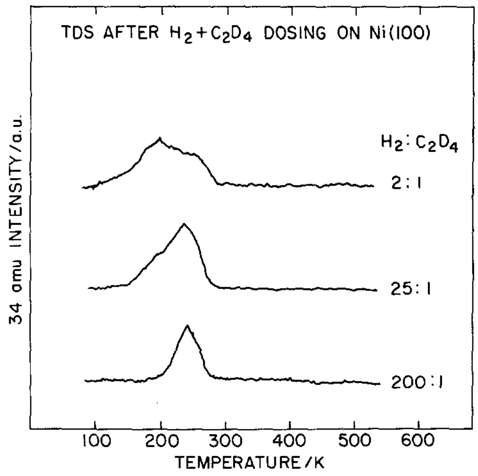

FIG. 3. TDS for 34 amu after sequential dosing of H_2 followed by C_2D_4 on Ni(100) at 90 K. The three traces correspond to three different relative coverages, as explained in the text.

shifted by about 10–20 K to lower temperatures.

Figure 2 also displays appreciable signals for 15, 17, 31, and 34 amu. The trace at 31 amu corresponds to a fragment of C_2D_3H stoichiometry, which is mainly due to the product of H–D exchange on chemisorbed ethylene. It displays a broad peak with maximum at 220 K and extra features at about 190 and 255 K. These peak maxima are at positions close to that for the molecular desorption, but the relative intensities are notoriously different, which indicates that exchange and desorption rates are comparable, and that exchange takes place to a greater extent between 190 and 220 K (the yield for exchanged ethylene is higher at 220 K). The total area of the 31-amu TDS trace is about 20% of that for the 32-amu signal, which shows that extensive exchange has taken place before molecular desorption. There could be a small contribution to the signal in the 30-amu trace due to multiple exchange, but if there is any it is not significant, since such spectrum mimics quite closely that obtained for 32 amu. Therefore, we propose that exchange occurs only once in each ethylene molecule. The TDS signal for 15 amu, corresponding to CDH fragments from ethylene cracking in the mass spectrometer ionizer, parallel the results from the 31 amu TDS; the small differences between the 15 and 31 amu TDS are due to the low quality of the 15 amu data because of the low sensitivity for this ion in the mass spectrometer.

Finally, the traces for 17 and 34 amu correspond to hydrogenation products. The 34-amu signal, which originates mainly from $C_2D_4H_2$ desorption, displays two peaks in the TDS, at 190 and 250 K. These two peaks are indicative of two regimes for ethylene hydrogenation. We have studied the relative importance of those two regimes as a function of $H_2:C_2D_4$ exposure ratios (Fig. 3). The dosings corresponding to the ratios in the figure (not corrected either by doser exposure enhancement or gas sensitivity) are 0.85 Langmuirs H_2 + 10.5 Langmuirs C_2D_4 (2 : 1), 10.5 Langmuirs H_2 + 10.5 Langmuirs C_2D_4 (25 : 1), and 10.5 Langmuirs H_2 + 1.3 Langmuirs C_2D_4 (200 : 1). From this figure it is clear that ethane forms first at 230 K, and only at higher C_2D_4 coverages the second peak grows in the low-temperature side (around 190 K). The 17-amu trace in Fig. 2 corresponds to CD_2H fragments (from cracking of partly deuterated ethane) and is similar to the 34-amu trace. The yield for ethane formation is fairly small, a few percent of the total chemisorbed ethylene. Since hydrogenation takes place between about 170 and 290 K, it also competes with both molecular desorption and H–D exchange reactions.

Figure 4 shows TDS for the case where ethylene was dosed prior to hydrogen. These results are clearly different from those in Fig. 2, which shows that the reaction of coadsorbed hydrogen and ethylene depends on the order in which the dosing is done. For the case where ethylene is adsorbed first, molecular desorption takes place in two well-defined peaks centered at 220 and 267 K. (see 16-, 30-, and 32-amu TDS). The high-temperature peak grows first at low ethylene coverages and shifts by about 10 K to lower temperatures with increasing dosages. The 15- and 31-amu TDS traces show two peaks which corresponds

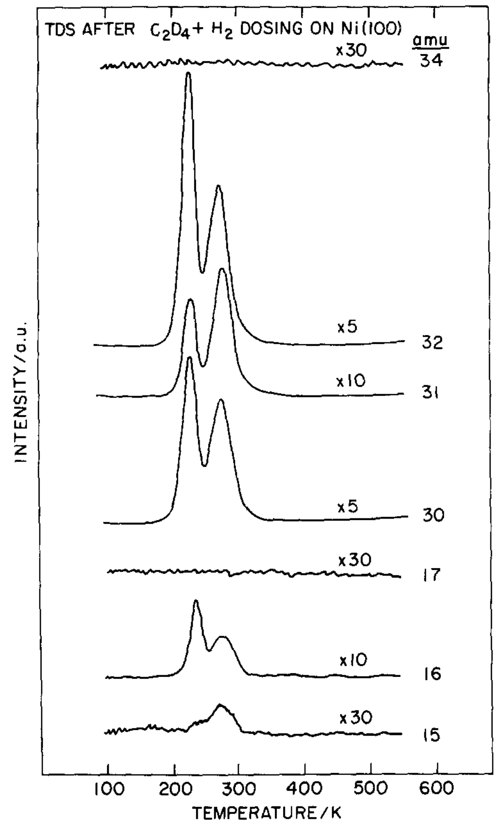

FIG. 4. TDS for 15, 16, 17, 30, 31, 32, and 34 amu after dosing sequentially a Ni(100) surface with 1.3 Langmuirs C_2D_4 followed by 0.85 Langmuirs at 90 K. Heating rate = 10 K/s.

to C_2D_3H desorption and which indicate that there is extensive H–D exchange competing with molecular desorption. As for the case in Fig. 2, the peaks are at the same temperatures as for molecular desorption but the exchange yield is higher in the high-temperature peak. The lack of any signal for the 17- and 34-amu traces indicates that no hydrogenation takes place under these conditions.

In order to characterize the coadsorption of ethylene with hydrogen in more detail we obtained high-resolution electron energy loss spectra for this system. The results from adsorption of hydrogen followed by C_2D_4 exposure at 90 K are shown in Fig. 5. The spectrum from 0.5 Langmuirs exposure of C_2D_4 alone is also shown for comparison. The vibrational assignment of the peaks is given in Table 1. The same spectra were obtained after annealing up to 170 K, but above 220 K no HREELS signal was detected within the noise of the spectra, indicating that most of the ethylene had already desorbed, either as C_2D_4, as exchanged ethylene, or as ethane.

DISCUSSION

The surface chemistry of ethylene when coadsorbed with hydrogen on Ni(100) was studied by TDS and HREELS. The presence of hydrogen on the surface greatly modifies the reactivity of adsorbed ethylene. The first thing to notice is that molecular desorption from adsorbed ethylene is enhanced when hydrogen is coadsorbed. Ethylene desorption from adsorbed ethylene on Ni(100) occurs for exposures above 1.3 Langmuirs. The TDS displays a broad peak centered around 250 K, which grows and shifts to 200 K at higher exposures (*4*). We have shown here that for the coadsorbed systems the molecular desorption

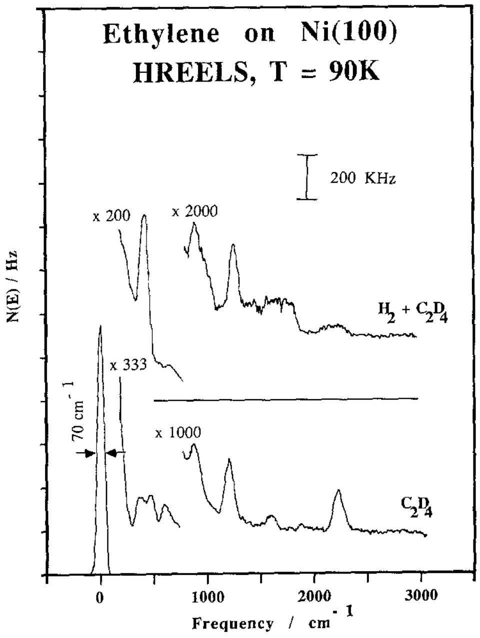

FIG. 5. HREEL spectra of chemisorbed C_2D_4 (0.5 Langmuirs) and of coadsorbed H_2 and C_2D_4 (0.85 and 10 Langmuirs, respectively) on Ni(100) at 90 K.

TABLE 1

Vibrational Mode Assignment for C_2D_4 in Different Environments (Vibrations in cm^{-1})

Mode	Gas phase (32)	$K[(C_2D_4)PtCl_3]$ (33)	0.5 Langmuirs C_2D_4/Ni(100) T = 90 K (4)	0.85 Langmuirs H_2 + 1.3 Langmuirs C_2D_4/Ni(100) T = 90 K
ν_{NiC} (stretch)	—	387	350, 450	425
ρ_{CD_2} (rock)	589[a]	536	595	580
τ_{CD_2} (twist)	720,[a] 780	811, 818	685	680
χ_{CD_2} (wag)	729,[a] 1010	450, 1021	860	800, 930
α_{CD_2} (scissor)	985, 1078[a]	978, 1067	1190	1290
ν_{CC} (stretch)	1517	1428	1575	1480
ν_{CD_2} (stretch)	2200[a]	2115	2205	2260
	2260	2185		
	2310	2219		
	2345[a]	2335		

[a] IR active bands.

yield is higher and occurs at lower ethylene coverages. Additionally, the TDS peak starts at lower temperatures when hydrogen is present, indicative of a weakening of the ethylene–metal chemisorptive bond. These TDS traces are quite complex in shape, which reveals the existence of several geometries for ethylene adsorption. In fact, TDS from coadsorption experiments are quite different depending on the order in which the dosing is done, which suggests that ethylene bonding is different for each case. We will come back to this point later.

The weakening of ethylene adsorption upon hydrogen predosing is supported by HREELS. The vibrational data indicates that C_2D_4 rehybridizes to a lesser extent on the surface when hydrogen is present (compared to gas phase). For instance, the nickel–ethylene stretching frequency is 450 cm^{-1} on clean nickel, but shifts to 425 cm^{-1} upon hydrogen preadsorption, indicating a weaker bond in the later case. In fact, a second peak at 350 cm^{-1} develops, suggesting that there are at least two distinct adsorption sites in the coadsorbed case. Most other peaks are seen at higher frequencies when hydrogen is also adsorbed on the surface. For example, the C–D stretch is seen at 2205 cm^{-1} on clean Ni, at 2260 cm^{-1} on hydrogen-presaturated nickel, and at 2200 and 2345 cm^{-1} in the gas phase. This is to be expected because they correspond to vibrations within the ethylene molecule, which are less affected by the metal if hydrogen is present.

We have observed extensive H–D exchange in C_2D_4 when coadsorbed with hydrogen. On the basis of the areas under the ethylene TDS peaks (31 vs 32 amu) we estimate the yield for exchange to be about 20–30% of the total chemisorbed ethylene. This yield increases at higher temperatures relative to molecular desorption, which points to the fact that the exchange has a higher activation energy than desorption, even though the rates are comparable for both pathways. The fact that TDS peaks are at the same position for both reactions seems to indicate that they are correlated in some way. Perhaps an exothermic step in the exchange provides excess energy localized on the surface, which could enhance the desorption of adjacent ethylene molecules. A similar mechanism has been suggested for the displacement of CO by hydrogen (*18*), in what has been called adsorption-assisted desorption. Additionally, only one hydrogen atom seems to be exchanged in each ethylene molecule, which would suggest a mechanism that involves the formation and rehydrogenation of vinyl as an intermediate. Vinyl groups do form from ethylene adsorbed alone on Ni(100) at about 170 K (*4–6*), below the temperature where exchanged ethylene desorbs, which is consistent with the proposed mechanism.

Ethylene hydrogenation also competes with both molecular desorption and H–D exchange. Ethylene self-hydrogenation has been reported to occur at high pressures on a number of supported metal catalysts, including nickel surfaces (*1*), and on Pt(111) even under UHV conditions (*10, 19, 20*). Hasse *et al.* studied the self-hydrogenation of ethylene on Ni(111) surfaces at pressures up to 0.1 mbar and determined that the probability for this reaction is about 3×10^{-4} (*12*). Under UHV, only molecular desorption and dehydrogenation have been seen on nickel surfaces (*4, 7, 21–23*). However, hydrogenation under vacuum is enhanced by hydrogen preadsorption. We have shown that the ethane yield can be increased by a factor of 50 if a platinum surface is saturated with hydrogen prior to ethylene adsorption (*10*). Here we report the same effect on Ni(100). While we see no ethane formation when ethylene is chemisorbed alone, or even when the surface is exposed to hydrogen after ethylene adsorption, there is appreciable ethane desorption in TDS experiments if hydrogen is dosed first (Figs. 2 and 3). We have shown by computer simulations that, on Pt(111), ethylene decomposition is required in order to provide the atomic hydrogen on the surface needed for ethane formation (*10*). This ethylene decomposition step is rate limiting, so if surface hydrogen is provided by other means (such as hydrogen preadsorption), hydrogenation takes place at lower temperatures. In fact, we found that, while ethylene self-hydrogenation has an activation energy of 18 kcal/mol (the same within experimental error as that for decomposition to ethylidyne and hydrogen), hydrogenation of ethylene in the presence of coadsorbed hydrogen only required 6 kcal/mol (*10*). Hasse *et al.* proposed a similar mechanism on Ni(111), in which some of the adsorbed ethylene decomposes to form acetylene and hydrogen and in which hydrogen is then incorporated into other ethylene molecules to form ethane (*12*). The fact that ethane desorption from chemisorbed ethylene alone is not seen on Ni(100) can be explained by kinetic arguments, by assuming that ethylene molecular desorption competes favorably against ethane formation. However, since the production of ethane depends on hydrogen surface coverage, its rate could be enhanced by hydrogen preadsorption to the point of being comparable to that for ethylene desorption. Our experiments show that this may be the case. The differences between our results on Ni(100) and those reported on Ni(111) can also be explained by the experimental conditions since the higher ethylene pressures used in Ref. (*12*) provide sufficient ethylene coverage at high temperatures so hydrogenation reactions can take place.

In the discussion given above we proposed that H–D exchange for ethylene on Ni(100) may take place through the formation of a vinyl intermediate, while hydrogenation, which needs to go through hydrogen incorporation steps, is much less favorable. An alternative explanation can be given based on an analogy with the ethylene chemistry on Pt(111). We have shown that ethylene coadsorbed with hydrogen on platinum surfaces produces ethyl groups, which immediately react through two competitive pathways to form either ethane or ethylene (*10, 34*). The rates for carbon–hydrogen bond-breaking and bond-forming on ethyl fragments have close values (*35*), and therefore comparable yields for hydrogenation and H–D exchange are observed. In the case of Ni(100) it could be possible that ethyl groups are formed as well, but that the rate for their dehydrogenation is much faster than for their hydrogenation, and therefore the H–D exchange yield is much larger than ethane formation. We are presently performing experiments using ethyl iodide (which forms ethyl moieties on the surface) in order to test this hypothesis.

The results reported here illustrate not only that preadsorbed hydrogen is needed for ethane formation, but also that the order of adsorption is crucial in determining the energetics and yields of the reactions involved. Ethane formation was only observed when hydrogen was dosed first; no hydrogenation occurs if the surface is presaturated with ethylene (compare Figs. 2 and 4). The areas under the hydrogen and ethylene TDS traces are comparable for both cases, indicating that the difference in reactivity is not due to a change in surface coverage. We can explain these results in terms of chemisorption geometries by using the available information on hydrogen and ethylene adsorption. LEED and helium diffraction data indicate that hydrogen chemisorption occurs on hollow sites (*24, 25*), forming disordered layers on Ni(100). The work function of the surface increases with hydrogen coverage due to charge transfer from the metal to the hydrogen atoms (*26*). Hydrogen diffusion occurs readily on Ni(100), the activation energy for such a process being only 4 kcal/mol for low hydrogen coverages (*27*), but the surface diffusion rate is greatly reduced at higher coverages and slows down even further in the presence of small amounts of coadsorbed gases (*28*). We can assume that hydrogen surface diffusion does not play an important role in ethylene hydrogenation under UHV conditions.

Ethylene chemisorption has also been studied extensively. The low-temperature adsorption on Ni(100) is believed to occur mainly by π-bonding (*4*), with the molecular plane tilted with respect to the surface by 50° (*6*). An ordered layer forms after 0.5 Langmuirs ethylene exposure at 80 K, and a $(\sqrt{2}x\sqrt{2})$ $R45°$ LEED pattern is obtained (*29*). The LEED results suggest that the ethylene saturation coverage is one-half, but XPS results have yielded lower values, on the order of one-third (*30*), which still represents a crowded surface. In contrast to the results for hydrogen adsorption, the surface work function decreases with ethylene coverage, implying that charge transfer from the molecule to the surface occurs, consistent with the picture of π-bonding (*31*).

The given information on hydrogen and ethylene chemisorption can be used to explain the results for ethane formation. Since diffusion of the surface species is negligible under our reaction conditions, coadsorption of hydrogen and ethylene must occur in an appropriate geometry in order for the hydrogenation reaction to take place. If hydrogen is dosed first, molecular H_2 dissociates and H atoms adsorb on the surface hollow sites. Ethylene then chemisorbs on top of this surface, perhaps on a side of a nickel atom, as its chemisorption geometry suggests. In this configuration hydrogen atoms are close to the ethylene molecule so they can react to form ethane. The proximity of both moieties on the surface can also explain the reduced heat of chemisorption for ethylene manifested by molecular desorption at lower temperatures, as mentioned earlier. On the other hand, if ethylene is chemisorbed first, hydrogen can only adsorb on the remaining free nickel surface, separated from the ethylene molecules, and this results in a spatial arrangement unfavorable for the hydrogenation. This explanation has been overly simplified and does not account for the different desorption peaks in the TDS, but explains the general trends observed and can be used to guide our thinking.

CONCLUSIONS

We have studied the hydrogenation and the H–D exchange of ethylene on Ni(100) surfaces and under UHV. Ethylene adsorption becomes weaker when hydrogen is coadsorbed, as manifested by an increase yield and a lower activation energy for molecular desorption compared to the case of starting from a clean nickel surface. H–D exchange takes place to an appreciable extent between ethylene and adsorbed hydrogen and competes with molecular desorption. Exchange occurs regardless of the order in which the gases are dosed, but the TDS results are quite different, indicating that the kinetics for such a reaction is sensitive to the chemisorption geometries of both reactants. Ethylene hydrogenation was also detected, but only if hydrogen was dosed prior to ethylene chemisorption. This result indicates that ethane formation is also very sensitive to the arrangement of the reactive moieties on the surface, and explains why ethylene self-hydrogenation has such a low reaction probability and is not seen on nickel, where molecular desorption takes place at very low temperatures.

ACKNOWLEDGMENT

The author thanks the Exxon Research and Engineering Co. for lending him the experimental apparatus.

REFERENCES

1. Horiuti, J., and Miyahara, K., "Hydrogenation of Ethylene on Metallic Catalysts. NSRDS-NBS 13, 1968.
2. Zaera, F., and Somorjai, G. A., *in* "Hydrogen Effects in Catalysis. Fundamentals and Practical Applications" (Z. Paál and P. G. Menon, Eds.), pp. 425–447. Dekker, New York, 1988.
3. Sheppard, N., *Annu. Rev. Phys. Chem.* **39,** 589 (1988).
4. Zaera, F., and Hall, R. B., *Surf. Sci.* **180,** 1 (1987).
5. Hall, R. B., Bares, S. J., DeSantolo, A. M., and Zaera, F., *J. Vac. Sci. Technol. A* **4,** 1493 (1986).
6. Zaera, F., Fischer, D. A., Carr, R. G., and Gland, J. L., *J. Chem. Phys.* **89,** 5335 (1988).
7. Zaera, F., and Hall, R. B., *J. Phys. Chem.* **91,** 4318 (1987).
8. Zaera, F., and Somorjai, G. A., *J. Amer. Chem. Soc.* **106,** 2388 (1984).
9. Beebe, T. P., Jr., and Yates, J. T., Jr., *J. Amer. Chem. Soc.* **108,** 663 (1986).
10. Godbey, D., Zaera, F., Yates, R., and Somorjai, G. A., *Surf. Sci.* **167,** 150 (1986).
11. Dalmai-Imelik, G., and Massardier, J., *in* "Proceedings, 6th International Congress on Catalysis, London, 1976" (G. C. Bond, P. B. Wells, and F. C. Tompkins, Eds.), pp. 90–100. The Chemical Society, London, 1977.
12. Haase, W., Günter, H.-L., and Henzler, M., *Surf. Sci.* **126,** 479 (1983).
13. Steininger, H., Lehwald, S., and Ibach, H., *Surf. Sci.* **123,** 264 (1982).
14. Sexton, B. A., *J. Vac. Sci. Technol.* **16,** 1033 (1979).
15. Hall, R. B., and DeSantolo, A. M., *Surf. Sci.* **137,** 421 (1984).
16. Gland, J. L., Shen, S., Zaera, F., and Fischer, D. A., *J. Vac. Sci. Technol. A* **6,** 2426 (1988).
17. Stenhagen, E., Abrahamsson, S., and McLafferty, F. W., Eds., "Registry of Mass Spectral Data." Wiley, New York, 1974.
18. Shen, S., Zaera, F., Fischer, D. A., and Gland, J. L., *J. Chem. Phys.* **89,** 590 (1988).
19. Steininger, H., Ibach, H., and Lehwald, S., *Surf. Sci.* **117,** 685 (1982).
20. Berlowitz, P., Megiris, C., Butt, J. B., and Kung, H. H., *Langmuir* **1,** 206 (1985).
21. Lehwald, S., and Ibach, H., *Surf. Sci.* **89,** 425 (1979).
22. Stroscio, J. A., Bare, S. R., and Ho, W., *Surf. Sci.* **148,** 479 (1984).
23. Demuth, J. E., *Surf. Sci.* **76,** L603 (1978).
24. Christmann, K., Behm, R. J., Ertl, G., Van Hove, M. A., and Weinberg, W. H., *J. Chem. Phys.* **70,** 4168 (1979).
25. Lee, J., Cowin, J. P., and Wharton, L., *Surf. Sci.* **130,** 1 (1983).
26. Christmann, K., Schober, O., Ertl, G., and Neumann, H., *J. Chem. Phys.* **60,** 4528 (1974).
27. George, S. M., DeSantolo, A. M., and Hall, R. B., *Surf. Sci.* **159,** L425 (1985).
28. Hall, R. B., private communication.
29. Horn, K., Bradshaw, A. M., and Jacobi, K., *J. Vac. Sci. Technol.* **15,** 575 (1978).
30. Koel, B. E., White, J. M., and Goodman, D. W., *Chem. Phys. Lett.* **88,** 236 (1982).
31. Demuth, J. E., and Eastman, D. E., *Phys. Rev. B* **13,** 1523 (1976).
32. Sverdlov, L. M., Kovner, M. A., and Krainov, E. P., "Vibrational Spectra of Polyatomic Molecules." Wiley, New York, 1974.
33. Nakamoto, K., "Infrared and Raman Spectra of Inorganic and Coordination Compounds." Wiley, New York, 1978.
34. Zaera, F., submitted for publication.
35. Zaera, F., *Surf. Sci.* **219,** 453 (1989).